Absence of Subharmonic Response in Vibrated Granular Systems under Microgravity Conditions

Jonathan E. Kollmer, Martin Tupy, Michael Heckel, Achim Sack, and Thorsten Pöschel
Institut für Multiskalensimulation, Friedrich-Alexander-Universität Erlangen-Nürnberg, 91052 Erlangen, Germany
(Received 21 October 2014; revised manuscript received 16 December 2014; published 19 February 2015)

By means of experiments in microgravity conditions, we show that granular systems subjected to sinusoidal vibrations respond either by harmonic or gaslike dynamics, depending on the parameters of the vibration, amplitude and frequency, and the container size, while subharmonic response is unstable, except for extreme material properties and particular initial conditions. The absence of subharmonic response in vibrated granular systems implies that granular dampeners cannot reveal higher-order resonances, which makes them even more attractive for technical applications. Extensive molecular dynamics simulations support our findings.

DOI: 10.1103/PhysRevApplied.3.024007

I. INTRODUCTION

Granular systems subjected to vibration reveal a plethora of interesting phenomena such as self-organized convection flows, e.g., Ref. [1], various segregation phenomena, e.g., Refs. [2,3], dynamical structure formation, e.g., Refs. [4–7], and interesting phase-transition phenomena, e.g., Refs. [8,9], just to name a few. To a large degree, these effects are influenced by gravity; therefore, in order to study these systems in the absence of gravity, experiments have been performed in parabolic flights, drop towers, and sounding rockets. Examples for such investigations concern shear flow, e.g., Refs. [10,11], cooling and clustering in granular gases [12–17], propagation of sound [18], Maxwell-demon effects [19], and violations of the energy equipartition in dilute granular systems [20–22]. A recent review can be found in Ref. [23].

When a container partly filled by granular material is sinusoidally agitated under conditions of weightlessness, distinct regimes of dynamical behavior have been predicted based on particle simulations [24,25]. In experiments in microgravity [26], it was found that the granulate reveals either gaslike behavior (uncorrelated particle dynamics) or harmonic dynamics, depending on the parameters of driving and the material properties, in agreement with the numerical predictions [25]. In particular, it was shown that the gas-regime and harmonic dynamics are fundamentally different with respect to the dissipation of energy due to inelastic particle collisions. The dissipated energy per unit time as a function of the parameters of driving as well as the basins of stability of both regimes can be explained up to quantitative agreement using a relatively simple model based on a one-particle description [26,27]. Interestingly, while the model description will allow also for subharmonic response, such behavior was never observed in hundreds of single experiments [26,28] as well as numerical simulations [24,25]. Therefore, in this paper, we raise the question if and under which conditions a subharmonic response is possible for a box filled by granular material and vibrated in microgravity.

The technical application behind our research is granular vibration dampeners. Essentially, such dampeners are containers (or cavities) partially filled by granular material. When subjected to vibration, dissipative particle collisions counteract the source of vibration, thus, attenuating the mechanical oscillation of an attached structure. Granular dampeners have a number of features which make them interesting for technical applications: They operate almost independently of the temperature, also in a harsh environment, and are free of maintenance due to the simplicity of their construction. Granular dampeners do not need any fixed anchor as a reservoir of momentum. There are several fields of applications of granular dampeners, such as attenuation of the vibration of mechanical tools and machinery [29], medical tools [30], sports equipment [31,32], turbine blades [33,34], break drums [35], metal cutting machines [36], antennas [37–39], bonding machines [40], and others. Granular dampeners were also considered for damping vibrations of the space shuttle engine [41,42]. As gravity tends to demobilize the granulate [43], granular dampeners work particularly well in applications where the acceleration due to gravity can be neglected as compared to the acceleration of the vibration. This scope includes, of course, applications in microgravity conditions, e.g., in spacecraft engineering. Thinking of futuristic applications, granular dampeners may be a suitable candidate for *in situ* resource utilization [44], as they can be easily manufactured from granular materials abundant on the Moon or Mars [45].

Unfortunately, in contrast to other types of dampeners, for granular dampeners, by now there is no reliable design rule which will allow an engineer to tailor a dampener to a specific application, e.g., characterized by typical amplitude and frequency of oscillation. Our research aims towards developing such design rules. By means of experiments, in combination with numerical simulation, we explain why, for realistic material parameters, the subharmonic response of a granulate to vibrational agitation is suppressed; thus, there are no higher-order resonances in the response of granular dampeners.

II. SYSTEM DESCRIPTION

We consider a rectangular box of size $L_x \times L_y \times L_z$ filled by N particles of mass m under vibration $x(t) = A\cos(\omega t)$. The clearance l_g is the difference between box length L_x and the width of the layer the granulate will form when packed (RCP) in a box of base area $L_y \times L_z$; see Fig. 1. From numerical simulations [24,25] as well as experiments [26], it is known that there are two different modes of dynamical behavior. For large amplitude $A \gg l_g$, we find the granulate in the "collect-and-collide" regime where all the material is collected during the inward stroke and, thus, forming a relatively densely packed layer at the wall of the container. The layer of particles leaves the wall collectively when the container passes the phase of maximal velocity; that is, the sinusoidal driving decelerates. The period is closed when the granulate impacts the opposite wall of the container, where the material is collected again; see Fig. 1(b). For a small amplitude $A \lesssim l_g$, the system behaves gaslike; in other words, the trajectories of the particles are uncorrelated due to the fact that they hit the driving wall at random phases [26].

The collective properties of these regimes are rather different: In the gas state, the dynamics of the particles is essentially decoupled from the periodic driving mechanism, except for a small fraction of particles populating the region close to the walls which is swept by the periodic motion of the wall. The interaction of these particles with the driving walls is just sufficient to balance the energy loss the gaseous bulk of the material due to dissipative particle-particle collisions. In contrast, in the collect-and-collide mode, when the particles impact the wall collectively, the system undergoes an inelastic collapse at the approaching wall due to a large number of collisions (see Refs. [46,47] for a detailed discussion). Therefore, twice per period, the kinetic energy corresponding to the relative velocity between the particles and the wall is dissipated. The great dissipative power of granular systems in this regime gave rise to their application as granular dampeners; see, e.g., Refs. [26,27,43,48]. Following the reasoning above, the system was described by an effective one-particle model,

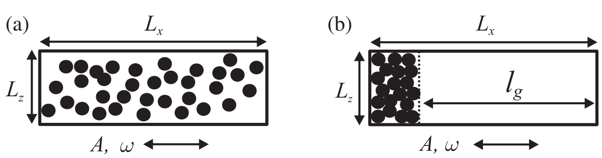

FIG. 1. Sketch of the system considered here, showing gaslike behavior (a) and collective motion (b). For further explanation, see the text.

where the granulate was represented by a single particle interacting with the walls at the vanishing coefficient of restitution $\varepsilon = 0$ [26]. In particular, one obtains a criterion for stability of the collect-and-collide regime: At the inward stroke, the material will lose contact with the wall at $t = 0$ when the acceleration of the sinusoidal motion changes its sign. The position of the quasiparticles is then $x_p(t) = A\omega t$. The position of the opposite wall is $x_w(t) = L_x + A\sin(\omega t)$. The collision takes place at time t_c when $x_w - x_p = L_x - l_g$. For stability, at t_c, the opposite wall must accelerate towards the impacting material to allow for the next "collect" phase, thus,

$$A\omega t_c = A\sin(\omega t_c) + l_g, \qquad \omega^2 \sin(\omega t_c) < 0. \tag{1}$$

For harmonic response $\omega t_c < 2\pi$, Eq. (1) has a solution if $A > l_g/\pi$ which is a necessary and sufficient condition for stability, independent of ω. Otherwise, for $A < l_g/\pi$, the synchronization condition is violated, and the system will enter the gas regime (see Ref. [26] for a full discussion).

However, while $A > l_g/\pi$ is the condition for a harmonic solution of Eq. (1), this equation has also subharmonic solutions [49],

$$2\pi n \le \omega t_c < (2n+1)\pi, \qquad n = 1, 2, \ldots, \tag{2}$$

corresponding to stability conditions

$$\frac{1}{2n}\frac{l_g}{\pi} > A > \frac{1}{2n+1}\frac{l_g}{\pi} \tag{3}$$

(see Fig. 2).

Although the single-particle model explained experiments up to quantitative agreement [26–28,50], the

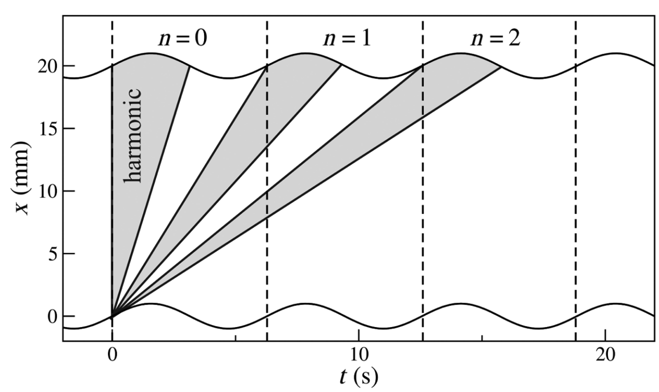

FIG. 2. Illustration of the stability condition of Eq. (1). The sinusoidal lines (not to scale) symbolize the motion of the container walls at $x = A\sin(\omega t)$ and $x = A\sin(\omega t) + l_g$, corrected by the clearance l_g. For stability of the collect-and-collide regime, the trajectory of the quasiparticle must not leave the shaded areas, thus, defining the valid intervals for the amplitude corresponding to the harmonic solution of Eq. (1) and subharmonic solutions of escalating order shown up to $n = 3$.

existence of subharmonic solutions of Eq. (1) contradicts previous results: In hundreds of single experiments and in numerical simulations [24,25], no sign of subharmonic response became apparent. From this finding, we conclude that the model description is still incomplete or insufficient. Therefore, we review the preconditions of the theory by means of an experiment.

III. EXPERIMENT

A polycarbonate box is partially filled by different amounts (mass m, particle number N) of steel beads (diameter 4 mm, material density 7.8 g/cm^3, Young's modulus 203.5 GPa) and driven by a linear actuator to perform sinusoidal oscillations of adjustable frequency ω and amplitude A. Table I summarizes the characteristics of our samples. To exclude the influence of gravity, the experiment is performed during a parabolic flight allowing for stable microgravity condition ($0 \pm 0.05g$) for time intervals of about 22 sec. Each experiment is repeated five times. The combinations of the applied driving amplitudes $A = 0.5$, 1.0, 2.0, 3.0, 4.0, 5.0 cm and frequencies $f = 0.5$, 1.0, 2.0, 4.0 Hz constitute, thus, an abundance of 120 single experiments. While observing the collect-and-collide regime for all systems fulfilling the stability condition for harmonic response, no sign of subharmonic response is found for systems fulfilling the condition for subharmonic stability (samples 1 and 4 at $A = 10$ cm). Instead, for systems not fulfilling the condition for harmonic response, the dynamics is always found gaslike, in contradiction with the model description.

The experiment is recorded by means of a video camera placed perpendicular to the direction of motion x at frame rate 240 frames/ sec and resolution of 448×336 pixels. To obtain a space-time representation of the granulate (Fig. 3) for each frame, we compute the average gray value in the plane perpendicular to the oscillation, thus, condensing the system's state at a certain time to a single line. Finally, these lines are stacked up to yield a space-time plot of the particle trajectories of the granulate and the container walls during the oscillatory motion. Figure 3 shows these plots for both the collective regime at different frequencies [Figs. 3(a)–3(d)] and an example of the gas regime [Fig. 3(e)].

While the model assumes that the particles undergo an inelastic collapse at the incoming wall and leave the wall collectively at velocity $v = A\omega$, Fig. 3 evidences a dispersion of the particle trajectories. In other words, in contrast to the model assumption, the collapse is incomplete, preserving a small amount of the particles' relative motion. Consequently, after detaching from the collecting wall, not all particles move at velocity $v = A\omega$, but some of them move faster since they carried over some kinetic energy from the previous period of oscillation. Finally, this dispersion invalidates the impact time t_c according to Eq. (1), but instead, t_c has to be replaced by a finite interval of time.

Note that the incompleteness of the collapse is a consequence of large frequency but not of insufficient inelasticity. The relevant part of the inward stroke $\omega t \in (2n, 2n+1)\pi$, $n = 0, 1, 2, \ldots$, is an accelerated motion. Therefore, the collapse will take place for any value of the coefficient of restitution, provided the inward stroke lasts long enough. This behavior is similar to the collapse of a particle (or a column of particles) jumping on a horizontal plane under gravity where the collapse occurs in finite time.

In Fig. 3, we see that all particles reach the opposite wall (or the surface of the sediment forming at the wall) before the wall starts to decelerate, that is, before $\omega t = \pi$. In particular, the particles collected in the vicinity of the wall (those who collide prior to others with the wall) lose essentially all their energy relative to the inwards accelerating wall. Therefore, the time when the wall starts to decelerate, at $\omega t = \pi$, the particles detach from the wall such that no particle can be slower than $A\omega$. While no particle may have smaller velocity than $A\omega$, particles may be faster (in absolute value). This higher velocity concerns, in particular, those particles which were collected immediately before $\omega t = \pi$, such that these particles did not suffer

TABLE I. Sample characteristics.

Sample	$L_x \times L_y \times L_z$ (mm^3)	m (g)	N	l_g (mm)	Ad (mm)
1	$100 \times 50 \times 50$	126.3	473	89.4	27 ± 3
2	$50 \times 50 \times 50$	135.3	507	38.7	7 ± 1
3	$50 \times 50 \times 50$	71.0	266	44.1	11 ± 1
4	$100 \times 50 \times 50$	63.8	239	94.7	20 ± 2

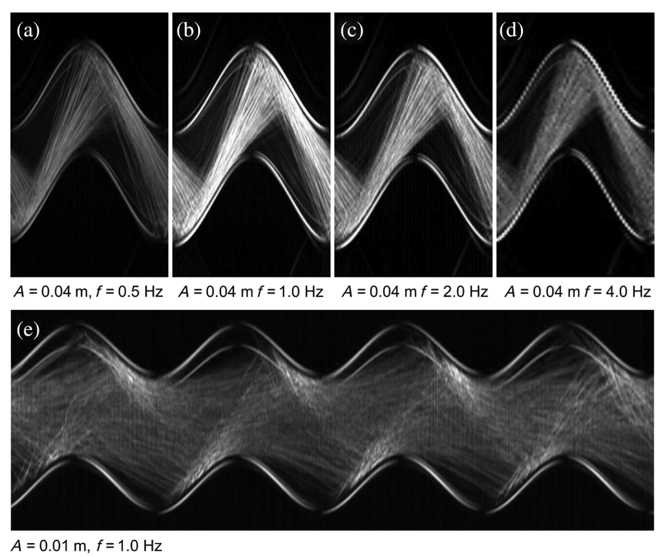

FIG. 3. Space-time plot of the experiment in the collect-and-collide regime (a)–(d) for different amplitudes and in the gaslike state (e). For all systems in the collective mode, we see clear dispersion of the trajectories.

too many collisions before the block of particles detaches from the wall. Therefore, plots of the type shown in Fig. 3 allow us to directly determine the interval of velocities of the ejected particles, $(v_{\mathrm{slow}}, v_{\mathrm{fast}}) = (A\omega, A\omega + \Delta v)$, where Δv depends only very weakly on the amplitude and approximately linearly on the frequency,

$$\Delta v = dA\omega, \qquad d > 0. \tag{4}$$

The constant d characterizes the incompleteness of the inelastic collapse and should, therefore, depend on the filling height and dissipative material parameters. For a detailed discussion, see Ref. [47]. The limited data set obtained in our parabolic flight experiments does not, however, allow us to determine these dependencies in detail. The experimentally measured $\Delta v/\omega = dA$ are given in the last column of Table I

IV. CRITICAL DISPERSION PARAMETER

From numerical simulations (see below and the Supplemental Material [51]), we find that even a small number of particles not joining the collective dynamics destabilizes the collect-and-collide regime. Therefore, we extend the criterion Eq. (1) by requiring that the synchronization condition must hold true for all particles, including the slowest and the fastest traveling at $v_{\mathrm{slow}} = A\omega$ and $v_{\mathrm{fast}} = A\omega + \Delta v$, respectively. Consequently, for stability, both equations

$$\begin{aligned} A\omega t_c &= A\sin(\omega t_c) + l_g, \\ A\omega t_c + \Delta v t_c &= A\sin(\omega t_c) + l_g, \end{aligned} \tag{5}$$

that is,

$$\omega t_c - \frac{l_g}{A} = \sin(\omega t_c), \tag{6}$$

$$(1+d)\omega t_c - \frac{l_g}{A} = \sin(\omega t_c), \tag{7}$$

must have solutions for the same basin of allowed amplitudes

$$A > \frac{l_g}{\pi}, \tag{8}$$

for harmonic response or

$$\frac{1}{2n}\frac{l_g}{\pi} > A > \frac{1}{2n+1}\frac{l_g}{\pi}, \tag{9}$$

for subharmonic response of order $n = 1, 2, 3, \ldots$, which poses a condition for d.

Consider first the harmonic response $0 \le \omega t_c \le \pi$. If Eq. (6) has a solution in this interval, Eq. (7) has also a solution for arbitrary $d \in (0, \infty)$; thus, for all system parameters, a harmonic response is possible.

The solution of Eq. (6) corresponding to subharmonic dynamics or order $n = 1, 2, \ldots$, belongs to the interval $2n\pi \le \omega t_c \le (2n+1)\pi$. Because of Eq. (5), the largest admissible value of Δv is adopted for $\omega t_c = (2n+1)\pi$ which corresponds to the largest possible value $d_{\max}^{(n)}$ corresponding to the order n for a given ratio l_g/A compatible with n; see Eq. (3). From Eq. (7) follows then

$$0 = (1 + d_{\max}^{(n)})2n\pi - \frac{l_g}{A}, \tag{10}$$

which has the solution

$$d_{\max}^{(n)} = \frac{l_g}{2n\pi A} - 1. \tag{11}$$

Summarizing these results and combining with the compatible intervals of A for harmonic and subharmonic solutions Eq. (3), we arrive at the maximum values for d that lead to stable collective motion:

$$d_{\max} = \begin{cases} \infty & \text{for } A > l_g/\pi, \\ \frac{l_g}{2n\pi A} - 1 & \text{for } \frac{1}{2n}\frac{l_g}{\pi} > A > \frac{1}{2n+1}\frac{l_g}{\pi}, \\ \text{no solution} & \text{else}, \end{cases} \tag{12}$$

with $n = 1, 2, \ldots$. Figure 4 shows $d_{\max}(A)$ for $l_g = 89$ mm corresponding to sample 1 (Table I). The envelope function of $d_{\max}(A)$,

$$d_{\max}^{\mathrm{env}}(A) = \frac{A\pi}{l_g - A\pi}, \tag{13}$$

diverges at $A = l_g/\pi$ in agreement with the existence of the harmonic response for all values of the dispersion parameter, d.

From Fig. 4, we understand immediately our experimental result (sample 1): No subharmonic response can be

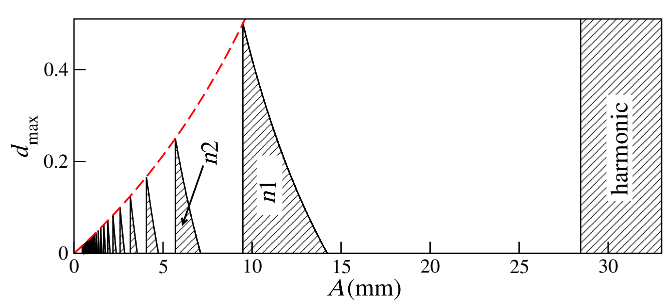

FIG. 4. Maximum admissible dispersion parameter as a function of amplitude as given by Eq. (12) for $l_g = 89$ mm (sample 1). For given d, the shaded regions indicate the values of A for which the subharmonic response of certain order n can be assumed. The condition $A > l_g/\pi$ for harmonic response is also shown; here, $d_{\max} \to \infty$. The dashed line shows the envelope given by Eq. (13).

found since the first subharmonic mode would be stable for $Ad \lesssim 4.8$ mm in a certain amplitude range, while in the experiment, we find $Ad = (27 \pm 3)$ mm. The same applies for the other samples specified in Table I.

V. INSTABILITY OF SUBHARMONIC MODES

Let us look to the scenario by which an existing subharmonic mode becomes unstable. To this end, we perform molecular dynamics (MD) simulations [52] of the system specified by Table I (sample 1). The dispersion parameter d describing the completeness of the inelastic collapse depends on the thickness of the layer of particles in the container $L_x - l_g$ determining the number of collisions occurring when the bulk of material collides with the wall and by the dissipative properties of particle collisions specified by the coefficient of restitution ε. Since $L_x - l_g$ is specified by our system setup, we choose ε to adjust d such that the subharmonic response becomes possible due to Eq. (12). Figure 5 shows the space-time plot corresponding to Fig. 3 but obtained from the MD simulation. For Fig. 5(a), the value of ε is chosen such that the resulting d allows for a subharmonic response due to Eq. (12). Figure 5(b) shows the system using slightly more elastic particles $\varepsilon = 0.2$, such that subharmonic motion is unstable. The transition from the unstable subharmonic regime to the stable gas regime starts with the desynchronization of single particles. Then the transition is accomplished after a few periods of oscillation. Initial conditions are chosen such that the particles form a dense layer at the box wall with velocity $A\omega$ in the direction of the agitation and zero velocity perpendicular to it. For animations showing the system in stable harmonic and subharmonic motion and the process of instability of subharmonic motion, see Ref. [51].

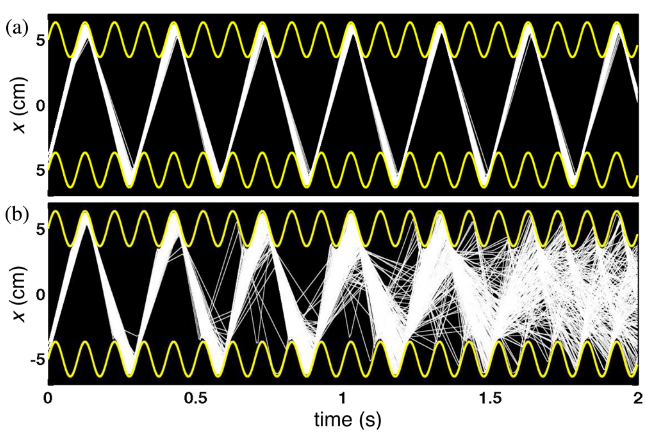

FIG. 5. Space-time plot obtained from a MD simulation of the system specified by Table I (sample 1). (a) Highly inelastic particles $\varepsilon = 0.02$ leading to $Ad \approx 3.0$ mm such that the subharmonic response is possible ($Ad_{\max}^{(n)} = 4.23$ mm) as given by Eq. (12), provided appropriate initial conditions. (b) Same as (a) but for $\varepsilon = 0.2$ resulting in $Ad \approx 5.5$ mm such that the subharmonic motion is unstable. See, also, Ref. [51].

Note that fulfilling the condition Eq. (12), e.g., by choosing a low-enough coefficient of restitution, is a necessary condition to obtain a subharmonic response but not necessarily sufficient: For the system shown in Fig. 5(a) revealing a stable subharmonic response for the initial conditions described above, we perform MD simulation starting with particle positions homogeneously distributed and velocities of random direction and absolute $v \in (-A\omega, A\omega)$. By scanning the interval of stable first-order subharmonic motion $A = (13, \ldots, 18)$ mm in steps of 0.5 mm and simulating over 200 periods for each value, we do not find any case of self-organized subharmonic motion, but in all cases, the gas state is assumed except when applying the boundary conditions as used in Fig. 5(a).

VI. CONCLUSION

A container partially filled by granular material responds to external sinusoidal vibration either by gaslike dynamics or by harmonic response while a subharmonic response is observed neither in experiments nor in numerical simulations. This behavior is not understood, in particular, since a model which reliably characterizes the stability of the gas and harmonic domains up to quantitative agreement with experimental data and successfully describes the dissipative properties of such a system does predict intervals of parameters where subharmonic dynamics is supposed to be stable. In conflict with these predictions, for these intervals of parameters, the gas regime appears stable. To solve the puzzle, by means of experiments performed in microgravity, we show that the assumption of an inelastic collapse taking place when the bulk of particles collectively impacts the wall is not justified in a strict sense. Instead, a certain dispersion parameter d should be applied, characterizing the residual relative velocities of the particles due to incomplete collapse. The resulting conditions for stability of subharmonic modes of escalating order require highly inelastic particle interaction, which explains that subharmonic modes have not been observed so far in experiments and simulations. Performing MD simulations, we evidence the stability of subharmonic motion, provided the stability criterion is fulfilled. We can show that even single particles desynchronizing from the collective motion due to a fluctuation can destabilize subharmonic motion. While the stability criterion Eq. (12) is a necessary condition for subharmonic motion, it remains unclear whether it is sufficient: In a large number of MD simulations using random initial conditions and with parameters fulfilling the stability criterion, we cannot find cases of spontaneous transitions to subharmonic motion. It remains unclear whether this lack is due to long transients or whether the initial conditions need to be chosen from a certain basin of attraction to allow the system to develop subharmonic dynamics.

The absence of subharmonic response of a container partially filled by granular material implies that there are no higher-order resonances in the dynamics of granular dampeners which makes such dampeners even more attractive for technical applications.

ACKNOWLEDGMENTS

We thank the European Space Agency (ESA) for funding the parabolic flight campaign and the German Science Foundation (DFG) for funding through the Cluster of Excellence "Engineering of Advanced Materials."

[1] J. A. C. Gallas, H. J. Herrmann, and S. Sokołowski, Convection Cells in Vibrating Granular Media, Phys. Rev. Lett. **69**, 1371 (1992).
[2] J. B. Knight, H. M. Jaeger, and S. R. Nagel, Vibration-Induced Size Separation in Granular Media: The Convection Connection, Phys. Rev. Lett. **70**, 3728 (1993).
[3] I. Aranson and L. Tsimring, *Granular Patterns* (Oxford University Press, New York, 2009).
[4] M. Faraday, On a peculiar class of acoustical figures, Phil. Trans. R. Soc. London **121**, 299 (1831).
[5] P. Umbanhowar, F. Melo, and H. L. Swinney, Localized excitations in a vertically vibrated granular layer, Nature (London) **382**, 793 (1996).
[6] C. Bizon, M. D. Shattuck, J. B. Swift, W. D. McCormick, and Harry L. Swinney, Patterns in 3D Vertically Oscillated Granular Layers: Simulation and Experiment, Phys. Rev. Lett. **80**, 57 (1998).
[7] D. Krengel, S. Strobl, A. Sack, M. Heckel, and T. Pöschel, Pattern formation in a horizontally shaken granular submonolayer, Granular Matter **15**, 377 (2013).
[8] A. Götzendorfer, C.-H. Tai, C. A. Kruelle, I. Rehberg, and S.-S. Hsiau, Fluidization of a vertically vibrated two-dimensional hard sphere packing: A granular meltdown, Phys. Rev. E **74**, 011304 (2006).
[9] M. Heckel, A. Sack, J. E. Kollmer, and T. Pöschel, Fluidization of a horizontally driven granular monolayer (to be published).
[10] M. Y. Louge, J. T. Jenkins, A. Reeves, and S. Keast, in *Proceedings of IUTAM Symposium on Segregation in Granular Flows* (Springer, New York, 2000), p. 103.
[11] N. Murdoch, B. Rozitis, K. Nordstrom, S. F. Green, P. Michel, T.-L. de Lophem, and W. Losert, Granular Convection in Microgravity, Phys. Rev. Lett. **110**, 018307 (2013).
[12] Y. Chen, M. Hou, P. Evesque, Y. Jiang, and M. Liu, Asymmetric velocity distribution in boundary-heating granular gas and a hydrodynamic description, AIP Conf. Proc. **1542**, 791 (2013).
[13] E. Falcon, R. Wunenburger, P. Evesque, S. Fauve, C. Chabot, Y. Garrabos, and D. Beysens, Cluster Formation in a Granular Medium Fluidized by Vibrations in Low Gravity, Phys. Rev. Lett. **83**, 440 (1999).
[14] S. Tatsumi, Y. Murayama, H. Hayakawa, and M. Sanoi, Experimental study on the kinetics of granular gases under microgravity, J. Fluid Mech. **641**, 521 (2009).
[15] Y. Grasselli, G. Bossis, and G. Goutallier, Velocity-dependent restitution coefficient and granular cooling in microgravity, Europhys. Lett. **86**, 60007 (2009).
[16] K. Harth, U. Kornek, T. Trittel, U. Strachauer, S. Höme, K. Will, and R. Stannarius, Granular Gases of Rod-Shaped Grains in Microgravity, Phys. Rev. Lett. **110**, 144102 (2013).
[17] E. Opsomer, F. Ludewig, and N. Vandewalle, Dynamical clustering in driven granular gas, Europhys. Lett. **99**, 40001 (2012).
[18] X. Zeng, J. H. Agui, and M. Nakagawa, Wave velocities in granular materials under microgravity, J. Aerosp. Eng. **20**, 116 (2007).
[19] E. Opsomer, M. Noirhomme, N. Vandewalle, and F. Ludewig, How dynamical clustering triggers Maxwell's demon in microgravity, Phys. Rev. E **88**, 012202 (2013).
[20] Y. P. Chen, P. Evesque, and M. -Y. Hou, Breakdown of energy equipartition in vibro-fluidized granular media in micro-gravity, Chin. Phys. Lett. **29**, 074501 (2012).
[21] M. Hou, R. Liu, G. Zhai, Z. Sun, K. Lu, Y. Garrabos, and P. Evesque, Velocity distribution of vibration-driven granular gas in Knudsen regime in microgravity, Microgravity Sci. Technol. **20**, 73 (2008).
[22] M. Leconte, Y. Garrabos, E. Falcon, C. Lecoutre-Chabot, F. Palencia, P. Evesque, and D. Beysens, Microgravity experiments on vibrated granular gases in a dilute regime: Non-classical statistics, J. Stat. Mech. (2006) P07012.
[23] Y. Huang, C. Zhu, and X. Xiang, Granular flow under microgravity: A preliminary review, Microgravity Sci. Technol. **26**, 131 (2014).
[24] M. N. Bannerman, J. E. Kollmer, A. Sack, M. Heckel, P. Mueller, and T. Pöschel, Movers and shakers: Granular damping in microgravity, Phys. Rev. E **84**, 011301 (2011).
[25] E. Opsomer, F. Ludewig, and N. Vandewalle, Phase transitions in vibrated granular systems in microgravity, Phys. Rev. E **84**, 051306 (2011).
[26] A. Sack, M. Heckel, J. E. Kollmer, F. Zimber, and T. Pöschel, Energy Dissipation in Driven Granular Matter in the Absence of Gravity, Phys. Rev. Lett. **111**, 018001 (2013).
[27] J. E. Kollmer, A. Sack, M. Heckel, and T. Pöschel, Relaxation of a spring with an attached granular damper, New J. Phys. **15**, 093023 (2013).
[28] A. Sack, M. Heckel, J. E. Kollmer, and T. Pöschel, Probing the validity of an effective-one-particle description of granular dampers in microgravity, Granular Matter, doi: (2014).
[29] J. C. Norcross, Dead-blow hammer head, U.S. Patent No. 3,343,576 (1967).
[30] M. Heckel, A. Sack, J. E. Kollmer, and T. Pöschel, Granular dampers for the reduction of vibrations of an oscillatory saw, Physica (Amsterdam) **391A**, 4442 (2012).
[31] R. Sommer, Sports equipment for ball games having an improved attenuation of oscillations and kick-back pulses and an increased striking force, U.S. Patent No. 5,454,562 (1995).
[32] S. Ashley, A new racket shakes up tennis, Mech. Eng. **117**, 80 (1995).
[33] R. Kielb, F. G. Macri, D. Oeth, A. D. Nashi, P. Macioce, H. Panossian, and F. Lieghley, Advanced damping systems for fan and compressor blisks, in *Proceedings of the National Turbine Engine High Cycle Fatigue Conference, Monterey, CA, 1999* (unpublished).
[34] A. L. Paget, Vibration in steam turbine buckets and damping by impacts, Engineering **143**, 305 (1937).

[35] Z. Xia, X. Liu, and Y. Shan, Application of particle damping for vibration attenuation in brake drum, Int. J. Vehicle Noise Vib. **7**, 178 (2011).

[36] D. I. Ryzhkov, Vibration damper for metal cutting, Eng. Digest **14**, 246 (1953).

[37] R. D. Rocke and S. F. Masri, Application of a single-unit impact damper to an antenna structure, Shock Vib. Bull. **39**, 1 (1969).

[38] S. S. Simonian, Particle beam damper, Proc. SPIE Int. Soc. Opt. Eng. **2445**, 149 (1995).

[39] W. Langer and G. Strienz, Schwingungsberuhigung hoher schlanker Bauwerke mit Hilfe von passiven Schwingungstilgern, IfL-Mitt. **30**, 46 (1991).

[40] K. W. Chan, W. H. Liao, M. Y. Wang, and P. K. Choy, Experimental studies for particle damping on a bond arm, J. Vib. Contr. **12**, 297 (2006).

[41] H. V. Panossian, Structural damping enhancement via non-obstructive particle damping technique, J. Vib. Acoust. **114**, 101 (1992).

[42] S. S. Simonian, Particle damping applications, in *45th AIAA/ASME/ASCE/AHS/ASC Structures Structural Dynamics and Material Conference*, Vol. 6, 4145 (2004), http://arc.aiaa.org/doi/abs/10.2514/6.2004-1906.

[43] C. Salueña, T. Pöschel, and S. E. Esipov, Dissipative properties of vibrated granular materials, Phys. Rev. E **59**, 4422 (1999).

[44] G. B. Sanders, K. A. Romig, W. E. Larson, R. Johnson, D. Rapp, K. R. Johnson, K. Sacksteder, D. Linne, P. Curreri, M. Duke, B. Blair, L. Gertsch, D. Bouchert, E. Rice, L. Clark, E. McCullough, and R. Zubrin, Results from the NASA capability roadmap team for in-situ resource utilization (ISRU), in *International Lunar Conference 2005; 7th ILEWG Conference on Exploration and Utilisation of the Moon (ICEUM7), 2005*, edited by R. Richards, C. Sallaberger, B. H. Foing, and D. Maharaj, http://sci.esa.int/Conferences/ILC2005/Manuscripts/SandersG-02-DOC.pdf.

[45] R. A. Wilkinson, R. P. Behringer, J. T. Jenkins, and M. Y. Louge, in *Space Technology and Applications International Forum-STAIF 2005*, American Institute of Physics Conference Series Vol. 746, edited by M. S. El-Genk (American Institute of Physics, College Park, Maryland, 2005), p. 1216.

[46] M. Sánchez, G. Rosenthal, and L. A. Pugnaloni, Universal response of optimal granular damping devices, J. Sound Vib. **331**, 4389 (2012).

[47] S. Luding, Ph.D. thesis, Universität Freiburg, 1994.

[48] M. Sánchez and L. A. Pugnaloni, Modelling of a granular damper, Mecanica Comput. **XXIX**, 1849 (2010).

[49] A. Mehta and J. M. Luck, Novel Temporal Behavior of a Nonlinear Dynamical System: The Completely Inelastic Bouncing Ball, Phys. Rev. Lett. **65**, 393 (1990).

[50] J. E. Kollmer, A. Sack, M. Heckel, F. Zimber, P. Müller, M. N. Bannerman, and T. Pöschel, Collective granular dynamics in a shaken container at low gravity conditions, AIP Conf. Proc. **1542**, 811 (2013).

[51] See the Supplemental Material at http://link.aps.org/supplemental/10.1103/PhysRevApplied.3.024007 for animations showing the system in stable harmonic and subharmonic motion and the process of instability of subharmonic motion.

[52] T. Pöschel and T. Schwager, *Computational Granular Dynamics* (Springer, Berlin, 2005).